NEW GEOMETRICAL-OPTIMIZATION APPROACH USING SPLINES FOR ENHANCED ACCELERATOR CAVITIES' PERFORMANCE

Mamdouh Nasr*, Sami Tantawi

SLAC National Accelerator Laboratory, CA, USA

Abstract

Over the past decades accelerator scientists made a huge effort in advancing the technology of particle accelerators, which lead to state-of-the-art fabrication techniques as well as simulation tools. Combining these advancements with the large boosting in computing speed provides large flexibility and motivation to investigate new accelerator geometries. In this paper, we describe a new optimization approach for the geometry of accelerating cells. This approach uses a set of control points with variable positions to control a non-uniform rational B-spline (NURBS), which describes the cavity shape.

INTRODUCTION AND DESCRIPTION

In this section, we describe a new optimization approach for the geometry of accelerating cells. This approach uses a set of control points with variable positions to control a nonuniform rational B-spline (NURBS) [1, 2], which describes the cavity shape. The positions of the control points are then optimized using differential-evolution optimization to maximize/minimize the defined optimization function. This function is defined by the user and depends on the cavity parameters such as the shunt impedance, wall losses, peak surface fields...etc

The set of control points used in our optimization for nose-shaped accelerator cells is shown in Fig. 1. The figure shows only a half-cell since we optimize for symmetric cells. Three sets of points control the cavity shape.

- First, four fixed points (black points) including the origin are defined using the cavity outer radius (b), iris radius (a), and cell width or periodicity (p). Typically, the iris radius is fixed, and the outer radius is used for frequency adjustments while the periodicity can be either fixed or added as a design variable.

- The second set of points are the green ones which only move horizontally (D0, D2 and D3) or vertically (D1). These points provide a guideline for the cavity cell shape. Point D0 is fixed vertically at the outer radius and provides extra control on the outer contour (upper quarter). It also forces the outer curvature to be convex. Point D1 and D2 are both fixed vertically at the iris radius and provides extra control on the nose shape. They also force the nose curvature to be concave. Point D3 is fixed horizontally at half the period edge minus the minimum separation between cells (t).
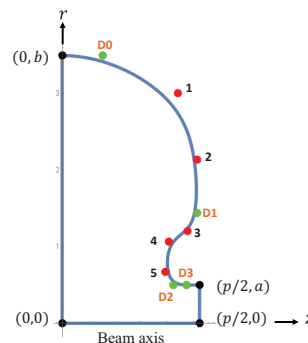
---
* mamdouh@slac.stanford.edu

Figure 1: The accelerating cavity cell is defined using a set of control points with variable positions to control a nonuniform rational B-spline (NURBS). The positions of the control points are then optimized to maximize/minimize a user-defined optimization function.

Table 1: The defined horizontal (H_{min} and H_{max}) and vertical (V_{min} and V_{max}) limits for each control point.

	H_{min}	H_{max}	V_{min}	V_{max}
Point D0	0	$0.5(p-t)$		
Point 1	Point D0$_x$	$0.5(p-t)$	Point D1$_y$	b
Point 2	Point 1$_x$	$0.5(p-t)$	Point D1$_y$	Point 1$_y$
Point D1			$a+2R_{min}$	$2b/3$
Point 3	xx_{min}	Point D1$_x$	$a+2R_{min}$	Point D1$_y$
Point 4	xx_{min}	Point 3$_x$	$a+R_{min}$	Point 3$_y$
Point 5	xx_{min}	Point 4$_x$	a	Point 4$_y$
Point D2	Point 5$_x$	$0.5p$		
Point D3	Point D2$_x$	$0.5p$		

- The last set of points (the red ones) can move horizontally and vertically. Points 1 and 2 control the outer contour while points 3-5 control the nose shape.

In order to produce acceptable shapes, we specified certain horizontal and vertical limits for each control point to avoid producing complex shapes. Also, we constrained points to move within the cavity boundaries defined by the outer radius and cell width. Moreover, because of mechanical limitation, we specified a minimum nose thickness of ($2R_{min}$) and a minimum horizontal separation between the noses (xx_{min}). We used these settings to create horizontal and vertical limits for each control point, which are listed in Table 1.

Once we defined the control points and their limits, we started setting up the optimization variables. We introduced three sets of variables. The first set (α_D) defines the positions of the green points; while the other two sets (α_x and α_y) define the horizontal and vertical positions of the red points, respectively. Also, we added another variable (α_p)

to control the periodicity within a range of $0.25\lambda_1$ to $0.5\lambda_1$, where λ_1 is the resonance wavelength of the first mode. We normalized each variable to a range from zero to one; Zero being the minimum horizontal/vertical limit and one being the maximum limit.

Figure 2 gives an illustration of how the position of Point 1 affect the overall curvature of the outer curvature of the cavity cell where $\alpha_{x,1}$ is assigned the values of 0.1, 0.5 and 0.9, respectively.
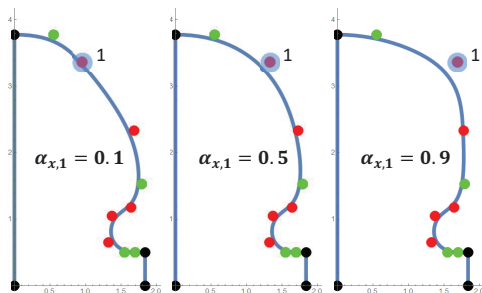

Figure 2: Illustration of how the position of Point 1 affect the overall curvature of the outer curvature of the cavity cell where $\alpha_{x,1}$ is assigned the values of 0.1, 0.5 and 0.9, respectively.

ACCELERATOR CELL OPTIMIZATION

In this section, we provide an optimization example for an S-band (2.856 GHz). We also used the following settings: an iris diameter of 5 mm, a minimum nose radius (R_{min}) of 0.05 cm and a minimum nose-separation (xx_{min}) of $p/2$, where p is the cell width/periodicity that will be included as an optimization parameter. We optimized for a maximum shunt impedance under the constraint of peak surface electric field-to-gradient ratio of two using the following optimization function:

$$\text{Optimization function} = \frac{R_{shunt}}{\text{Max}\left[\frac{E_{surf}}{G}, 2\right]} \quad (1)$$

where E_{surf} is the electric field at the cavity surface.

The differential-evolution optimizer gets the value of the optimization function at different points in the optimization space, then it starts narrowing down the search range until it converges to an optimized design. Figure 3 shows the value of the optimization function, shunt impedance and field-to-gradient ratio versus each step of the differential-evolution optimization. This shows how the optimizer narrows down the variables' range until it converges nicely to a maximized shunt impedance with field-to-gradient ratio of two. Figure 4 shows snapshots from the development of the accelerator cell shape at different simulation steps at the optimization process. We can see that the optimization started from some starting point and kept developing until it reached the optimum cavity shape under the defined constraints.

Our optimized single-mode design has a shunt impedance of 113 MΩ/m which is 10% higher than the one obtained
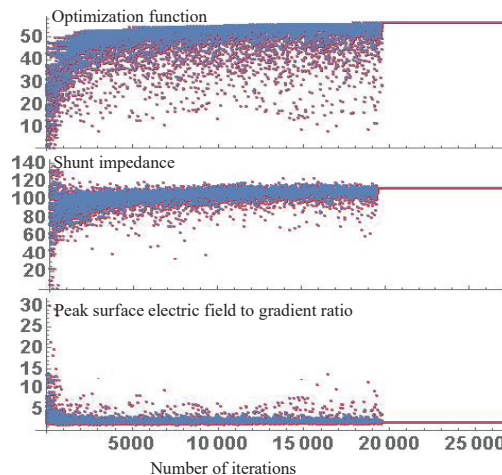

Figure 3: The value of the optimization function, shunt impedance and field-to-gradient ratio versus each step of the differential-evolution optimization.
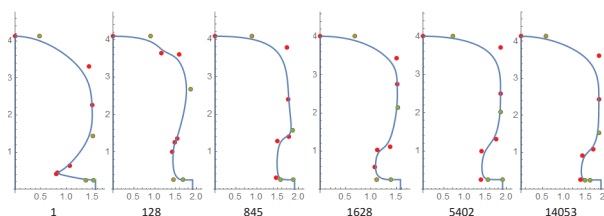

Figure 4: Snapshots from the development of the accelerator cell shape at different simulation steps at the optimization process. The number below each shape is the simulation index.

using conventional circular shapes. Figure 5 shows (a) the optimized cavity shape with the control points final positions as well as the normalized electric field distribution inside the cavity and (b) the electric and magnetic fields over the surface normalized to the average accelerating-gradient. It is worth noting that the cavity nose is perfectly shaped to have a very flat and smooth electric field distribution over the surface. The cavity outer dimensions and simulated accelerating-parameters are summarized in Table 2.

Table 2: Summary of the cavity outer dimensions and accelerating parameters. The peak fields are calculated for average gradient of 100 MV/m.

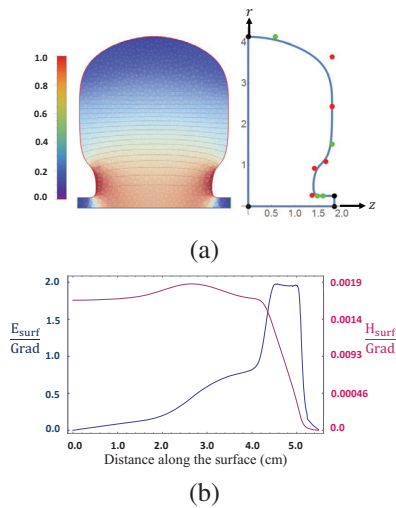|	
Frequency	2.586 GHz
a	0.25 cm
b	4.13 cm
p	3.67 cm
R_{shunt}	113 MΩ/m
Peak E_{surf}	200 MV/m
Peak H_{surf}	0.2 MA/m
S_c [3]	4.25 W/μm²
Surface Loss	3.26 MW

(a)

(b)

Figure 5: (a) the optimized cavity shape with the control points final positions as well as the normalized electric field distribution inside the cavity and (b) the electric and magnetic fields over the surface normalized to the average accelerating-gradient.

CONCLUSION AND FUTURE WORK

The availability of the fast simulation tool and new manufacturing techniques adds a huge flexibility in the accelerator cells design. In this work we described a new geometrical optimization approach that uses a set of control points to control the cavity shape and optimizes for higher shunt impedance and lower surface fields. This approach can be used in the optimization of other accelerating components like electron guns, dual-mode accelerator cells...etc for a higher efficiency and thus enhanced performance. This optimization technique can also be extended and used for superconducting structures resulting in lower surface magnetic fields in the accelerator cells.

REFERENCES

[1] L. Pirgl and W. Tiller, *Book of Nurbs*, ser. Book of Nurbs. Springer, 1995, no. v. 1. [Online]. Available: https://books.google.com/books?id=mJGUAAAACAAJ

[2] [Online]. Available: http://reference.wolfram.com/language/ref/BSplineFunction.html

[3] A. Grudiev, S. Calatroni, and W. Wuensch, "New local field quantity describing the high gradient limit of accelerating structures," *Physical Review Special Topics-Accelerators and Beams*, vol. 12, no. 10, p. 102001, 2009.